



The shifts in microbial interactions and gene expression caused by temperature and nutrient loading influence *Raphidiopsis raciborskii* blooms

Baohai Zheng^a, Ling Zhou^a, Jinna Wang^a, Peichang Dong^a, Teng Zhao^a, Yuting Deng^a, Lirong Song^b, Junqiong Shi^a, Zhongxing Wu^{a,*}

^a Key Laboratory of Eco-environments in Three Gorges Reservoir Region (Ministry of Education), Chongqing Key Laboratory of Plant Ecology and Resources Research in Three Gorges Reservoir Region, School of Life Sciences, Southwest University, Chongqing, 400715, PR China

^b State Key Laboratory of Freshwater Ecology and Biotechnology, Institute of Hydrobiology, Chinese Academy of Sciences, Wuhan, 430072, PR China

ARTICLE INFO

Keywords:

Global warming
Eutrophication
Microbial interactions
Raphidiopsis raciborskii
Cyanobacterial bloom

ABSTRACT

Climate change and the trophic status of water bodies are important factors in global occurrence of cyanobacterial blooms. The aim of this study was to explore the cyanobacteria–bacterial interactions that occur during *Raphidiopsis raciborskii* (*R. raciborskii*) blooms by conducting microcosm simulation experiments at different temperatures (20 °C and 30 °C) and with different phosphorus concentrations (0.01 mg/L and 1 mg/L) using an ecological model of microbial behavior and by analyzing microbial self-regulatory strategies using weighted gene coexpression network analysis (WGCNA). Three-way ANOVA revealed significant effects of temperature and phosphorus on the growth of *R. raciborskii* ($P < 0.001$). The results of a metagenomics-based analysis of bacterioplankton revealed that the synergistic effects of both climate and trophic changes increased the ability of *R. raciborskii* to compete with other cyanobacteria for dominance in the cyanobacterial community. The antagonistic effects of climate and nutrient changes favored the occurrence of *R. raciborskii* blooms, especially in eutrophic waters at approximately 20 °C. The species diversity and richness indices differed between the eutrophication treatment group at 20 °C and the other treatment groups. The symbiotic bacterioplankton network revealed the complexity and stability of the symbiotic bacterioplankton network during blooms and identified the roles of key species in the network. The study also revealed a complex pattern of interactions between cyanobacteria and non-cyanobacteria dominated by altruism, as well as the effects of different behavioral patterns on *R. raciborskii* bloom occurrence. Furthermore, this study revealed self-regulatory strategies that are used by microbes in response to the dual pressures of temperature and nutrient loading. These results provide important insights into the adaptation of microbial communities in freshwater ecosystems to environmental change and provide useful theoretical support for aquatic environmental management and ecological restoration efforts.

1. Introduction

Global climate change and eutrophication pose significant threats to the structure and function of freshwater ecosystems, resulting in severe challenges for freshwater ecosystem services (Polazzo et al., 2022). This global and persistent threat is expected to further worsen in the future based on the Fifth Assessment Report (AR5) of the Intergovernmental Panel on Climate Change (IPCC) (Stocker, 2014; Mammides, 2020). In response to climate change and eutrophication pressures, the frequency and magnitude of cyanobacterial blooms around the world are predicted to increase and even expand to include a wider geographic range for

some cyanobacterial taxa (Freeman et al., 2020). The toxins produced by the dominant bloom-forming cyanobacteria pose considerable risks to drinking water and ecosystem services, particularly in developing countries (Mohamed, 2016), and even to human health (Mammides, 2020). Therefore, there is growing concern that climate change and eutrophication influence the underlying processes leading to cyanobacterial bloom formation, which is very important for water resource management and freshwater ecosystem protection.

To date, many studies have shown that cyanobacterial blooms are related to water quality parameters, i.e., nitrogen and/or phosphorus concentrations, light, temperature, pH, and turbidity (Huisman et al.,

* Corresponding author.

E-mail address: wuzhx@swu.edu.cn (Z. Wu).

<https://doi.org/10.1016/j.watres.2024.122725>

Received 19 June 2024; Received in revised form 28 October 2024; Accepted 29 October 2024

Available online 30 October 2024

0043-1354/© 2024 Elsevier Ltd. All rights reserved, including those for text and data mining, AI training, and similar technologies.

2018). Traditionally, increasing nutrient concentrations are considered key factors responsible for promoting cyanobacterial blooms (Luerling and Faassen, 2012), whereas recent studies have indicated that warmer temperatures are also important drivers of blooms. For example, Anneville et al. (2005) reported that warmer winter temperatures, in addition to phosphorus concentrations, were the main drivers of changes in phytoplankton composition according to more than 25 years of monitoring in European peri-alpine lakes. O'Brien et al. (2009) reported that temperature controls the rates of enzymatic reactions, photosynthesis and biosynthesis in algal cells and directly affects algal proliferation (Kehoe et al., 2015). However, there are conflicting results about the relative importance of nutrients and temperature in driving cyanobacterial blooms. Studies by Paerl and Huisman (2008) suggested that warmer temperatures are more important than increasing nutrients in driving the formation of cyanobacterial blooms. Conversely, Rigosi et al. (2014) argued that cyanobacterial blooms are driven primarily by nutrient loading rather than climate change effects. Modeling simulations have shown that the synergistic interaction between temperature and nutrients may be responsible for cyanobacterial blooms (Elliott, 2012), but how these two factors interact in different cyanobacterial taxa remains unknown.

Recently, biotic factors such as microbes have attracted attention because they also play potential contributing roles in cyanobacterial bloom formation (Gerphagnon et al., 2015). Microbes are crucial components of freshwater ecosystems, contributing to the biogeochemical cycling of C, N, and P in such systems (Newton et al., 2011). Direct or indirect interactions between cyanobacterial blooms and microbial communities have been widely reported (Brauns et al., 2022). For example, cyanobacteria can provide habitats for other microbes (Bouma-Gregson et al., 2019). Moreover, changes in cyanobacterial abundance can alter microbial communities, resulting in increased structural vulnerability of the microbial community in aquatic environments due to phylogenetic clustering (Wang et al., 2020). On the other hand, the interaction between primary producers and bacteria affects the physiological functions of both parties and shapes ecosystem diversity. (Amin et al., 2015). Studies have identified highly interconnected "hub species" in microbial networks that serve as bridges between microbes and their hosts (Ling et al., 2016). Some heterotrophic bacteria may benefit from cyanobacterial blooms (Shao et al., 2014). In addition, some microeukaryotes (protists and zooplankton) may play important functional roles in the processing of cyanobacterial blooms (Liu et al., 2019). This finding indicates that the interactions between cyanobacteria and microbial communities are diverse, i.e., mutual or competitive (Du et al., 2022). Despite significant efforts to reveal the molecular mechanisms underlying microbial interactions (Saleem et al., 2019), it is challenging to detect and quantify the interactions of each microorganism in the highly complex ecosystem of aquatic environments.

By combining behavioral ecology and game theory, Jiang et al. (2019) developed methods to quantify and characterize different types of microbial interactions in any large ecological community, including mutualistic, antagonistic, exploitative, and altruistic interactions. These models have been validated and applied in a range of experiments in medicine (Jiang et al., 2021), botany (He et al., 2021), microbiology (Li et al., 2022), and environmental science and ecology (Du et al., 2022). For example, He et al. (2021) used this model to find structural differences in patterns of bacterial–fungal interactions and microbe complexity. Using a model, Du et al. (2022) reported that environmental changes promote cyanobacterial blooms, resulting in cyanobacteria being aggressive and antagonistic to other microorganisms. Studies have shown that microbial interactions can influence cyanobacterial properties (Kong et al., 2023), community assembly (Hu et al., 2022), material cycling (Isabwe et al., 2018), and bloom formation (Du et al., 2022). Despite significant efforts in previous studies to reveal the molecular mechanisms underlying microbial interactions (Saleem et al., 2019), the integrated effects of environmental change and the dynamics

arising from the interaction networks of microbial communities on cyanobacterial bloom cycles in aquatic ecosystems remain an open question.

The main aims of this study were to elucidate how changes in microbial communities exposed to climate change and nutrient loading impact cyanobacterial blooms and to elucidate the underlying ecological interactions. To address these objectives, shifts in microbial communities and ecological interactions during a notorious *R. raciborskii* bloom were characterized. This cyanobacterium spans different climates from tropical zones to temperate regions (Burford et al., 2016), and its toxins have been associated with several cases of human poisoning and animal death (Ohtani et al., 1992). Although many studies have proposed this species' strategies for adaptation, i.e., flexible strategies for acquiring phosphorus (Bai et al., 2014), nitrogen (Willis et al., 2016), and other dissolved minerals (Briand et al., 2002), as well as for coping with different light intensities (Everson et al., 2011) and temperatures (Zheng et al., 2023), none of these traits can clearly explain why the invasion or bloom formation of *R. raciborskii* has been so widespread thus far. Herein, we hypothesized that i) temperature and nutrient loading alter microbial communities (H1); ii) the synergistic effects of temperature and nutrient loading further alter the occurrence of *R. raciborskii* blooms (H2); and iii) shifts in microbial interactions and functional gene expression in related metabolic pathways caused by temperature and nutrient loading are responsible for *R. raciborskii* blooms (H3). Therefore, microcosm simulation experiments were conducted to test the effects of increasing temperatures and nutrient levels on the natural phytoplankton communities of subtropical eutrophic systems. Specifically, we tested the effects of changes in temperature (ambient annual mean temperature, 20 °C; high temperature, 30 °C) and phosphorus concentration (low, 0.01 mg/L; high, 1 mg/L) on microbial composition and functional response.

2. Materials and methods

2.1. Experimental design and microcosm establishment

Our experimental system consisted of 12 plexiglass tanks (the outside of the tank was covered with black plastic around the perimeter and bottom), each 0.4 m long, 0.3 m wide and 0.35 m high. These microcosms were used to create two climate scenarios, a high-temperature scenario (30 °C) and a low-temperature scenario (20 °C); these scenarios are consistent with the average annual temperatures of the aquatic ecosystems in the region (Ou-yang et al., 2022; Zheng et al., 2024) as well as the temperature tolerance range of *Raphidiopsis raciborskii*, which ranges from 19 °C to 40 °C, with an optimal range of 29 °C to 32 °C (Sinha et al., 2012). Two nutrient concentrations were also simulated, including a high phosphorus concentration (1 mg/L) and a low phosphorus concentration (0.01 mg/L); these conditions modeled the upper and lower limits of the phosphate concentration in the Nanpeng Reservoir, respectively.

In situ water and sediments were collected from an important drinking water reservoir, the Nanpeng Reservoir, upstream of the Huaxi River, which is a major tributary of the Three Gorges Reservoir in China. A total of 450 L of water was collected from five sampling locations at three depths (surface: 0.5 m below the surface, middle layer: 2 m below the surface, and bottom layer: 0.5 m above the sediment) to generate a mixed water sample. A Peterson grab sampler was also used to collect 1 m³ of sediment from the bottom of the reservoir at five different sampling locations. The collected water and sediment samples were immediately transported to the laboratory for processing. The sediment samples were homogenized and then evenly distributed to a thickness of 0.05 m at the bottom of the 12 tanks after being sieved through a 10-mesh screen to remove stones and other debris. The in situ water samples were filtered through a 20- μ m plankton mesh to remove large vegetation fragments and avoid the uncontrolled introduction of zooplankton and vertebrates. All the water samples were then mixed,

and qualitative and quantitative analyses of cyanobacterial species were performed (Table S1). The well-mixed 450-L water samples were each divided into two equal parts. The phosphorus treatments were mended with a K_2HPO_4 solution (40 mg/L) and with BG11-A5/20 medium as a source of vitamins and trace metals (Rippka et al., 1979), yielding final phosphorus concentrations of 1 mg/L and 0.01 mg/L, respectively. Water samples for each phosphorus concentration were then randomly distributed into six tanks, with the water depth set to 0.25 m. Finally, twelve tanks were placed in four constant temperature incubators (RXZ-430E, Dongnan Instruments, China). Incubations were maintained on a 14-hour light/10-hour dark cycle at $35 \mu\text{mol quanta m}^{-2} \text{s}^{-1}$ for 30 days. Samples were collected every two days. There were three replicates of each of the four treatments in the experiment: low phosphorus and low temperature (LL), low phosphorus and high temperature (LH), high phosphorus and low temperature (HL), and high phosphorus and high temperature (HH), with three replicates for each treatment (Fig. S1).

2.2. Phytoplankton analysis

The phytoplankton sample (1 L) was fixed by adding 15 mL of Lugol reagent, and after 48 h of settling through a split funnel in a dark indoor environment, the supernatant was removed, and 30 mL of the concentrated sample was retained for phytoplankton community analysis. Phytoplankton taxa were identified and counted in plankton counting chambers (20 mm \times 20 mm, 0.1 mL, Pusen, China) containing 100 μL of concentrated algal solution with a Nikon ECLIPSE Ci microscope (Nikon, Japan) at $400 \times$ magnification (Hu and Wei, 2006). Each sample was counted twice to ensure that the variation was less than 15 %, and two results were averaged to determine phytoplankton density (cells L^{-1}); in cases where variation was 15 % or greater, a third cell count was performed. According to the cyanobacteria bloom grade evaluation standard (ANZECC, 2000), an algal density $< 2.0 \times 10^6$ cells/L corresponded to no obvious bloom, whereas algal densities $\geq 2.0 \times 10^6$ cells/L, $\geq 1.5 \times 10^7$ cells/L and $\geq 1 \times 10^8$ cells/L were defined as slight bloom, mild bloom, and severe bloom conditions, respectively. Therefore, we defined an algal density of $\geq 2.0 \times 10^6$ cells/L as the mid-bloom stage (MB). The sample before the MB, in which the algal density was $< 2.0 \times 10^6$ cells/L, was defined as the pre-bloom stage (PB), and the sample after the MB, with an algal density $< 2.0 \times 10^6$ cells/L, was defined as the late-bloom stages (LB).

2.3. DNA extraction, library construction, metagenomic sequencing and functional annotation

Total genomic DNA was extracted from water samples via the MagAttract Power® Soil Pro DNA Kit (Qiagen, Hilden, Germany) according to the manufacturer's instructions. The concentration and purity of the extracted DNA were determined with TBS-380 and NanoDrop2000, respectively. The quality of the extracted DNA was evaluated on a 1 % agarose gel. Further details on DNA extraction, PCR conditions, sequence quality control, and genome assembly are available in Supplementary Information Texts S2 to S3. The raw reads were deposited in the NCBI Sequence Read Archive (SRA) database (accession number: PRJNA1097773).

2.4. Statistical analyses

Alpha diversity indices, including the Chao1 (species richness) and Shannon indices (species diversity, considering abundance and evenness), were calculated using the Mothur cloud platform (Schloss et al., 2009). Statistical analyses were performed using R version 4.2.2. Three-way ANOVA was performed to evaluate the main and interactive effects of temperature, phosphorus concentration, and bloom period on algal density. All three factors and their interactions were examined simultaneously in the same model, meaning that the analysis considers

the main effects and interactions together rather than conducting independent ANOVAs for each factor. Prior to analysis, the algal density data were subjected to square root transformation to meet normality assumptions. The residuals were checked with the Shapiro-Wilks test, and the Levene test was used to check the homogeneity of variances. Similarly, before conducting one-way ANOVA on alpha diversity indices to evaluate differences among groups (LL, LH, HL, HH), normality was checked with the Shapiro-Wilk test, and homogeneity of variances was checked with the Levene test. Post-hoc comparisons for both algal density and alpha diversity indices were performed using Tukey's HSD test (*emmeans* package) to examine significant interactions and differences between groups. Statistical significance was determined at $P < 0.05$. Pie charts and bar charts were generated in Origin 2022 (Origin Lab Inc., Northampton, MA, USA). For beta diversity analysis, non-metric multidimensional scaling (NMDS) was performed using the Bray-Curtis dissimilarity index, which is appropriate for ecological data characterized by high-dimensionality and nonlinear relationships. For the results of the NMDS analyses, the R values (reflecting the relative magnitude of between-group and within-group differences) and corresponding p values were calculated via analysis of similarities (ANOSIM) to test whether these differences were significant. NMDS and ANOSIM were performed using the *vegan* package in R 4.2.2.

To examine the relationships between species within the bacterioplankton community, molecular ecological network analyses (MENs) were performed via genus-level relative abundance data for each sampled taxon. Only genera with a relative abundance greater than 0.1 % were considered. Significant correlations between bacterioplankton species were identified via Spearman correlation coefficients, considering only those with coefficients > 0.7 or < -0.7 . The significance of these correlations was assessed via the Benjamini-Hochberg method to adjust p values ($P_{\text{adjust}} < 0.05$) to control for the frequency of false discoveries. Gephi (0.10.1) was used to visualize the MENs, and the *igraph* package in R 4.2.2 was used to calculate network topological parameters such as node (n), edge (L), degree, eigenvector centrality, average neighbor degree, and betweenness centrality in R 4.2.2. (Csardi and Nepusz, 2006).

Core nodes in molecular ecological networks (MENs) are characterized on the basis of their within-module connectivity (Z_i) and between-module connectivity (P_i). The connectivity metrics of the network nodes are calculated using the *igraph* package in R 4.2.2. The Z_i - P_i plot function from the *ggplot2* package is subsequently used to visualize and categorize the topological roles of nodes into four different categories, following the methodology outlined by Zheng et al. (2024). Specifically, $Z_i > 2.5$ and $P_i < 0.62$ indicate that module hubs exhibit substantial connectivity within a module. $Z_i < 2.5$ and $P_i > 0.62$ indicate that connectors are significantly connected between two modules. $Z_i > 2.5$ and $P_i > 0.62$ indicate that network hubs have elevated connectivity throughout the entire MEN, whereas $Z_i < 2.5$ and $P_i < 0.62$ suggest that peripherals lack significant connectivity within a module or between modules.

We selected the top 500 relative abundances of cyanobacteria and non-cyanobacterial bacteria to construct interaction networks using microbial behavioral network (MBN) models (Jiang et al., 2019), which classify interactions into four types: mutualism, antagonism, aggression, and altruism. The detailed methods for constructing these models are available in Supplementary Information Text S4.

To investigate the co-expression of functional genes in planktonic bacterial communities and identify their core functions at different temperatures and phosphorus concentrations, we performed WGCNA using the *WGCNA* package in R4.2.2 (Langfelder and Horvath, 2008). The detailed methods used for WGCNA can be found in Supplementary Information Text S5. Core functions were identified on the basis of the KEGG annotation and WGCNA results. Differential gene and enzyme testing and visualization of the screened hub metabolic pathways were performed on the Majorbio cloud platform (www.majorbio.com). The enzymes and genes involved in the metabolic pathways were examined

using a t-test between multiple groups of samples to analyze the significance of differences between groups. The abundances of the pathways and test results are then marked on the pathway map.

3. Results

3.1. Dynamics of the bacterioplankton community

During the entire experimental cycle, microscopic data on the algal densities of *R. raciborskii* revealed that *R. raciborskii* bloom events occurred in all the treatment groups, but there were significant

differences in the density of *R. raciborskii* among the treatment groups with different temperatures and phosphorus concentrations at the mid-bloom (MB) and late-bloom (LB) stages ($P < 0.05$, Fig. 1a). Specifically, the HL and LH groups presented moderate blooms, with maximum algal densities of 4.72×10^7 cells/L and 1.52×10^7 cells/L, respectively, whereas the LL and HH groups presented milder blooms, with maximum densities of 8.16×10^6 cells/L and 3.49×10^6 cells/L, respectively. Three-way ANOVA (Table S2) revealed significant effects of temperature ($P < 0.001$), phosphorus concentration ($P < 0.001$), and bloom period ($P < 0.001$) on *R. raciborskii* density. Additionally, significant interactions between temperature and phosphorus concentration were

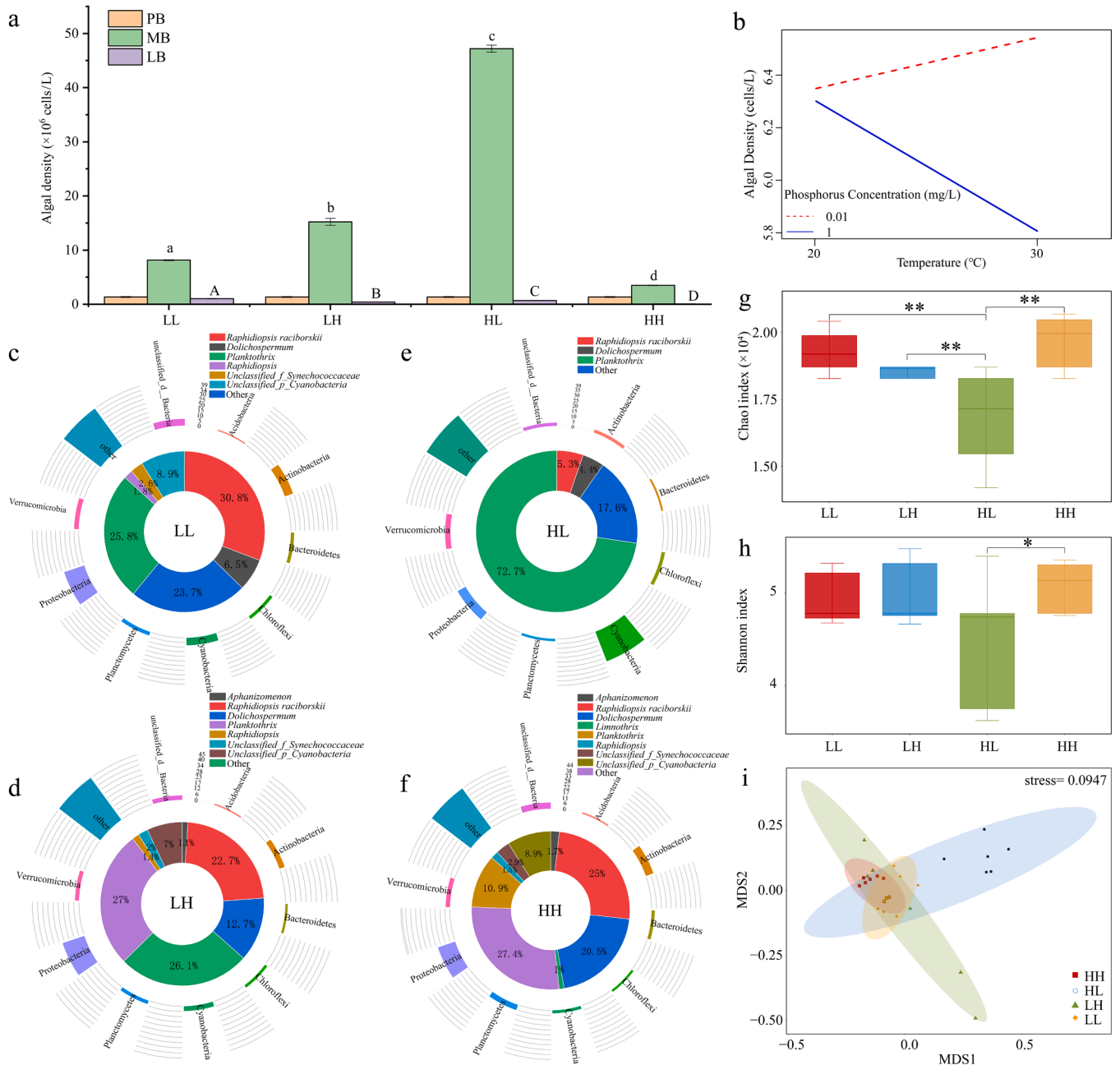


Fig. 1. Composition and diversity of the bacterioplankton community in the LL, LH, HL, and HH treatment groups. (a) Algae densities at different bloom stages in the four treatment groups. The small letters indicate significant differences in the mean algal density among the treatments at the mid-bloom (MB) stage. Similarly, mean algal densities at the late-bloom (LB) stage were compared across treatments, and capital letters indicate significant differences. No significant differences in algal density were detected at the pre-bloom (PB) stage (one-way ANOVA, $P < 0.05$). (b) Interaction effect of temperature and phosphorus concentration on algal density. The algal density data were subjected to log-transformation (log10). (c-e) Bacterioplankton composition at the phylum level (outer circle) and cyanobacterial composition at the genus level (inner circle) for the different treatment groups. The genera of cyanobacteria in the inner circle are annotated in the upper right corner of each circle. (f-g) α -Diversity of bacterioplankton. (i) NMDS ordination based on the Bray-Curtis distance for different treatments.

detected ($P < 0.001$). Under low-phosphorus conditions, elevated temperatures promoted algal growth, whereas under high-phosphorus conditions, increased temperatures inhibited algal growth (Fig. 1b).

A total of 159 phyla, 265 orders, 475 orders, 999 families, 4094 genera and 59,159 species were identified through taxonomic annotation of species through the Nonredundant Protein Sequence Database (NR). At the phylum level, taxa differed significantly among the LL, LH, HL and HH groups, with relative abundances greater than 1 % for each (Fig. 1c–f). Except for the HL group, which consisted of 8 phyla, the other groups consisted of the same 9 phyla, with Proteobacteria and Actinobacteria ranking highest in terms of relative abundance (Figs. 1c, d, and f). In the HL group, cyanobacteria had the highest abundance, followed by proteobacteria, whereas actinobacteria were absent (Fig. 1e).

The relative abundance of cyanobacteria was 7.06 %, 4.58 %, 29.70 %, and 2.90 % in the LL, LH, HL, and HH groups, respectively, with *R. raciborskii* being the most abundant species in the LL and HH groups and *Planktothrix* dominating in the LH and HL groups (Fig. 1c–f). The relative abundances of *R. raciborskii* in cyanobacteria and bacterioplankton were 30.79 % (LL), 22.72 % (LH), 5.30 % (HL) and 25.02 % (HH) and 2.17 % (LL), 1.04 % (LH), 1.57 % (HL) and 0.73 % (HH), respectively. Species diversity ($F = 5.35$, $P < 0.01$) and richness ($F = 7.33$, $P < 0.001$) in the HL group showed significant differences compared to other treatment groups (Fig. 1g and h), which was supported by the NMDS and ANOSIM results ($P < 0.05$, Fig. 1i, Table S3).

3.2. Bacterioplankton interaction networks

In the symbiotic network of bacterioplankton, which simulates variations in temperature and phosphorus, the numbers of nodes and edges varied among the treatment groups (Fig. 2). Specifically, the LH and HH groups presented greater numbers of nodes and edges than did the LL and HL groups, with the LH group having the highest number of nodes and edges ($n = 520$ and $L = 15,467$), which increased by 20.65 % and 89.25 %, respectively, compared with the LL group, which had the fewest number of nodes ($n = 460$), and the HL group, which had the fewest number of edges ($L = 8173$). Proteobacteria exhibited the highest relative abundance in the LH and HH groups, whereas cyanobacteria were most abundant in the LL and HL groups. Additionally, the LL and LH groups presented slightly higher percentages of positive correlations for potential bacterioplankton interactions than did the HL and HH groups. Linear fit analysis revealed that network degree was significantly positively correlated with eigenvector centrality, average neighbor degree, and betweenness centrality (log) ($P < 0.001$, Fig. S3).

A total of 22 hub species, including 5 module hubs and 17 connectors, were identified across the networks (Fig. 2, Table S4), which belonged to Acidobacteria (1 species), Chloroflexi (1 species), Cyanobacteria (6 species), Planctomycetes (1 species), Proteobacteria (8 species), unclassified_d_bacteria (1 species), and Verrucomicrobia (4 species). Specifically, all 5 module hubs were present only in the HL group, and all belonged to cyanobacteria.

The MBNs revealed that the LH and HH groups had significantly more nodes and edges than the LL and HL groups did (Fig. 3). The relationships within communities were predominantly altruistic, although there were differences among the groups (Fig. S4). Proteobacteria and cyanobacteria were typically the taxa with the highest relative abundances among the four relationships. Proteobacteria were usually the dominant taxon for mutualism and antagonism (except for HL, which was the dominant taxon for mutualism, Fig. 3c), whereas cyanobacteria were the dominant taxon for aggression and altruism. Interestingly, in the LL and HH groups, cyanobacteria were more engaged in aggression (Fig. 3a and d), whereas non-cyanobacteria were more active in other relational behaviors in the LH and HL groups (Fig. 3b and c). Tracking the hub species via Zi-Pi analysis revealed that almost all the genes were classified as altruistic, except for one module hub in the HL group belonging to *Raphidiopsis*, which was simultaneously classified as

mutualism, antagonism, and altruism (Table S4).

To further elucidate the detailed interaction process and intensity between cyanobacteria and non-cyanobacterial bacteria at different temperatures and phosphorus concentrations, dMBNs were reconstructed for different treatment groups (Fig. 4). The results revealed that mutualistic and antagonistic relationships among all the treatment groups were dominated by Proteobacteria and Cyanobacteria (Fig. 4a–c), except for the HH group, where Bacteroidetes also played a significant role alongside proteobacteria (Fig. 4d). Notably, the relative abundance of non-cyanobacteria under both mutualistic and antagonistic conditions was consistently greater than that of cyanobacteria in the LL, LH, and HL groups and was significantly greater in the HH group (Fig. 4d).

Furthermore, in the aggression and altruism networks, although proteobacteria and Cyanobacteria nodes presented the highest degrees, significant differences in degree, in-degree, and out-degree were observed between cyanobacteria and non-cyanobacteria in all the treatments (Fig. 4a–d Bottom stacked bar chart of MBNs). In aggressive interactions, non-cyanobacteria consistently showed higher relative abundance and in-degree than did cyanobacteria (more than 79 %). Conversely, with the exception of the HL group, cyanobacteria demonstrated higher out-degrees, indicating a more prominent role in aggressive behavior in all the treatments. Notably, cyanobacteria also displayed altruism toward both non-cyanobacterial bacteria and themselves in all the treatments. Specifically, cyanobacteria showed altruism towards non-cyanobacteria as well as toward themselves (HH > LL > LH > HL) under all the treatments (Fig. 4a–d bottom stacked bar chart of the MBNs). Proteobacteria in the LL, LH and HH groups and Proteobacteria and Actinobacteria in the HL group were all major beneficiaries (Tables S5 and S6).

3.3. Gene expression of bacterioplankton

Our results revealed significant enrichment across all treatment groups for six primary KEGG metabolic pathways, with notable differences in the read counts for each classification (Fig. S5). (Fig. S5). WGCNA segregated all the bacterioplankton genes into eight modules at a soft power (β value) of 14 and a merged cutoff height of 0.25 (Figs. 5a and S6). Significant correlations were detected between the functional genes and these modules across the four treatments (Fig. 5b), with the LL, LH, HL and HH treatments being significantly positively correlated with brown ($R = 0.407$, $P < 0.05$), yellow ($R = 0.524$, $P < 0.01$), turquoise ($R = 0.853$, $P < 0.001$) and black ($R = 0.441$, $P < 0.05$) colors, respectively (Fig. 5c). These findings were supported by module membership and gene significance (MM-GS) analysis (Fig. 5d).

Visual network analysis linked these four pivotal modules to the metabolic pathways specific to each treatment group (Fig. 5e). The LL group was enriched for replication and repair, cell growth, and death-related tertiary pathways, including DNA replication, base excision repair, homologous recombination, nucleotide excision repair, mismatch repair, etc. The LH group was enriched for metabolic pathways related to oxidative stress, such as glutathione metabolism, oxidative phosphorylation, etc. The HL treatment affects photosynthesis and energy metabolism pathways, including photosynthesis, photosynthesis - antenna proteins, ubiquinone and other terpenoid quinone biosynthesis, lipoic acid metabolism, starch and sucrose metabolism, etc. The HH treatment was significantly related to cell signaling metabolic pathways, such as lysosomes, the sphingolipid signaling pathway, Janus kinase signal transducer and activator of transcription, etc. (Tables S7 and S8).

Further analysis of the intergroup variations in genes or enzymes involved in these pathways (Fig. 6) revealed significant enrichment of DNA replication genes, such as *POLA1* and *pol*, in the LL group, whereas LH treatment resulted in increased expression of enzymes involved in glutathione metabolism, such as spermine synthase and 5-oxoprolinase (ATP-hydrolyzing), ornithine decarboxylase, and other enzymes

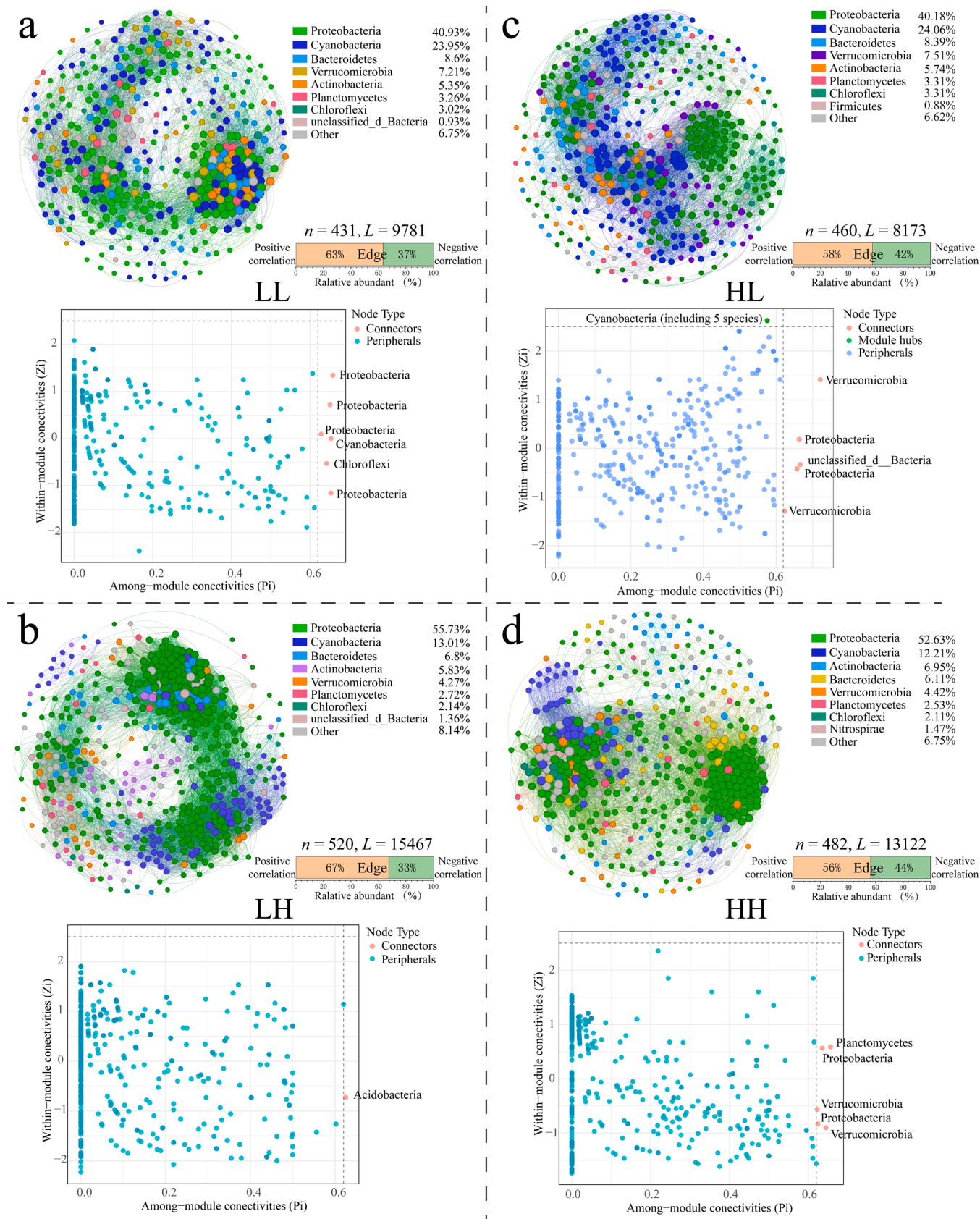


Fig. 2. Molecular ecological network of bacterioplankton. (a-d) Molecular ecological network of different treatment groups at the species level (top), bar chart of the proportion of positive and negative correlations in the lateral relationship (middle) and Zi-Pi plots (bottom).

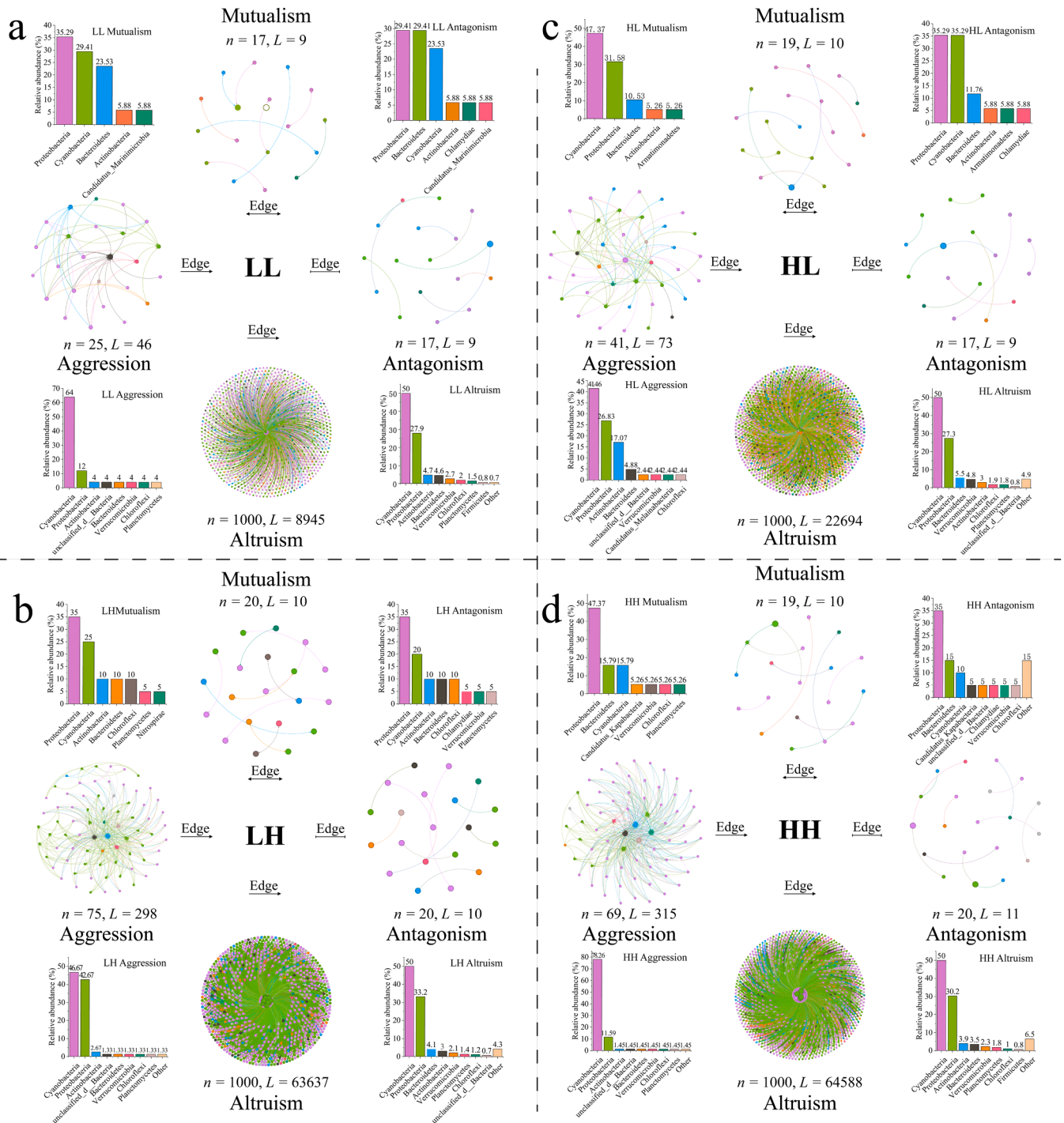


Fig. 3. Microbial behavioral networks and their ecological relationships with bacterioplankton in the LL, LH, HL, and HH groups. (a-d) MBN analysis for the LL, LH, HL, and HH treatments, respectively. The top in the interaction network of each treatment group mutualism network symbolizes microbial cooperation by two arrows; right: antagonism network signifies the mutual conflict among microbes by bidirectional T-shaped edges; left: aggression network specifies how a microbe preys upon others by edges with single arrows; bottom: altruism network illustrates how one microbe benefits others by an edge with a single arrow. The bar graphs represent the relative abundance of phylum-level bacterioplankton for each of the four relationships in each network, and the colors of the nodes in the interaction network correspond one-to-one to the color of each bar graph representing the interaction of the same species in the network. The size of the nodes represents the degree of each species at the genus level.

involved in glutathione metabolism. HL treatment upregulated genes related to photosynthesis, including ferredoxin-NADP⁺ reductase and the cytochrome b6-f complex iron-sulfur subunit (*psbP*, *psb27*, *psb28*, *psb28-2*, and *petJ*). In the HH group, genes related to lysosomes, such as *NEU1*, *NAGLU*, *AGA*, *aspG* and other genes, were notably upregulated (Table S9). Additionally, an analysis of genes related to carbon,

nitrogen, phosphorus, and sulfur cycling revealed that all treatment groups primarily engaged in processes such as the reductive citrate cycle (Arnon-Buchanan cycle), organic nitrogen metabolism, and transport and assimilatory sulfate reduction (Figs. S7–S10, Tables S10–S13). Notably, the LH treatment resulted in significantly greater gene expression for pathways involved in anaerobic ammonium oxidation,

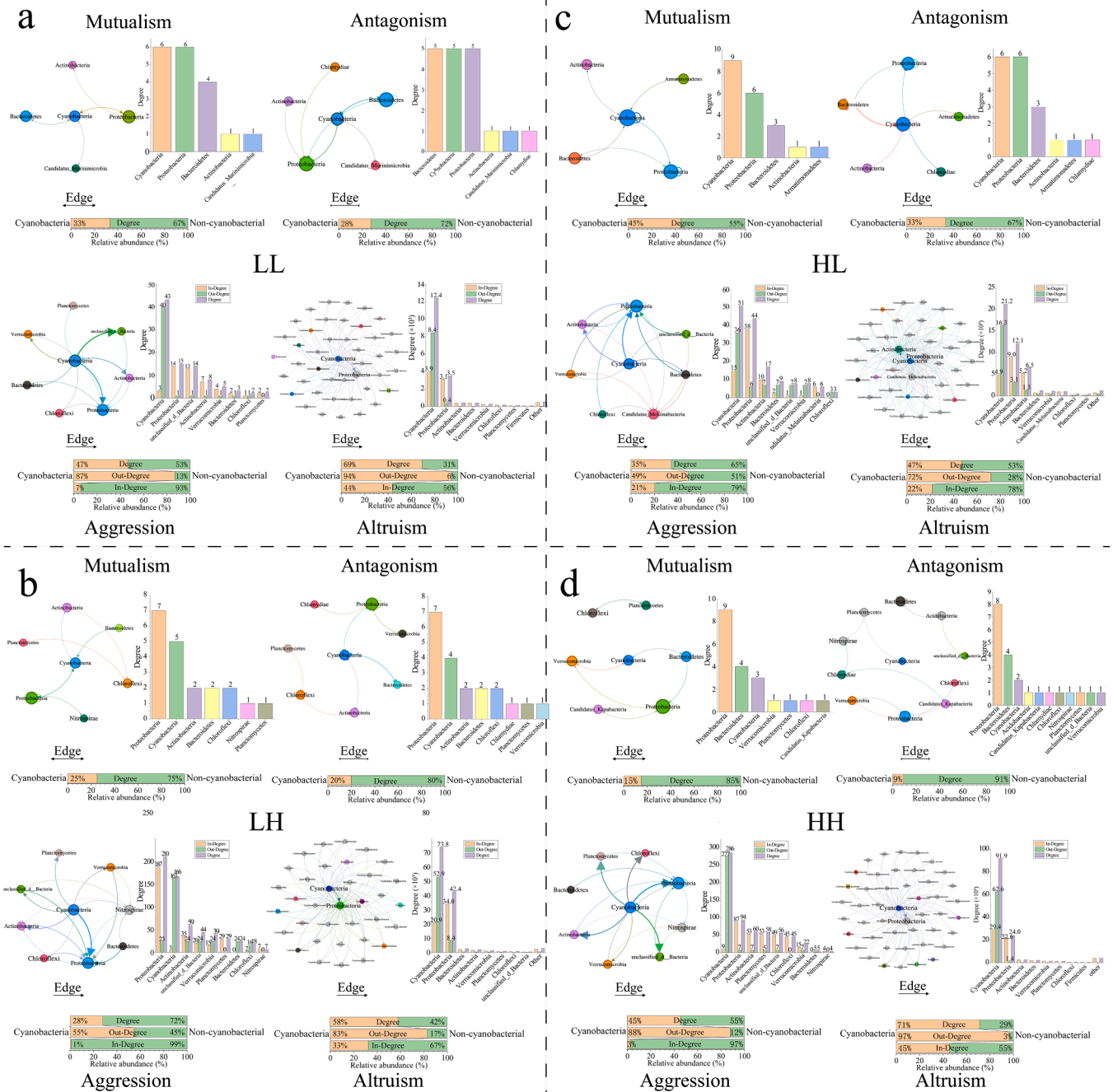


Fig. 4. Number of degrees, in-degrees and out-degrees of microbial behavioral networks. (a-d) Degree of microbial behavioral networks in the LL, LH, HL, and HH treatment groups, respectively. The size of the circle in each network diagram represents the degree of the species; the width of the edge represents the width of the weight (the number of connections between two nodes by the arrows, reflecting the number of species interacting with each other at the species level). The bars on the right side of the network diagram represent the number of degrees, in-degrees, and out-degrees for aggression and altruism (at the gate level). The stacked bar charts below the network diagrams represent the relative abundance of cyanobacteria and non-cyanobacterial bacteria in terms of all degrees.

denitrification, nitrogen transport, polyphosphate degradation, and both assimilatory and dissimilatory sulfate reduction, with phosphate transporter expression markedly greater in LL ($P < 0.05$, Tables S14–S17).

4. Discussion

4.1. Temperature and nutrient loading alter microbial communities

Metagenomic annotation of planktonic bacteria revealed that during the bloom period, heterotrophic microbial communities were

dominated by Proteobacteria, Planctomycetes, Bacteroidetes, Verrucomicrobia, and Actinobacteria (Fig. 1), which is consistent with previous research (Te et al., 2023). Increasing evidence suggests that Proteobacteria and Bacteroidetes are major components of the bacterial communities of the freshwater phycosphere (Smith et al., 2021). In our multivariate analysis, we found that the effects of temperature and nutrient loading on microbial communities are reflected not only in relative species abundance, but also in changes in community structure and function through altered interactions among different species. For example, network analysis indicated that Proteobacteria and Cyanobacteria were the taxa with the highest relative abundances among the

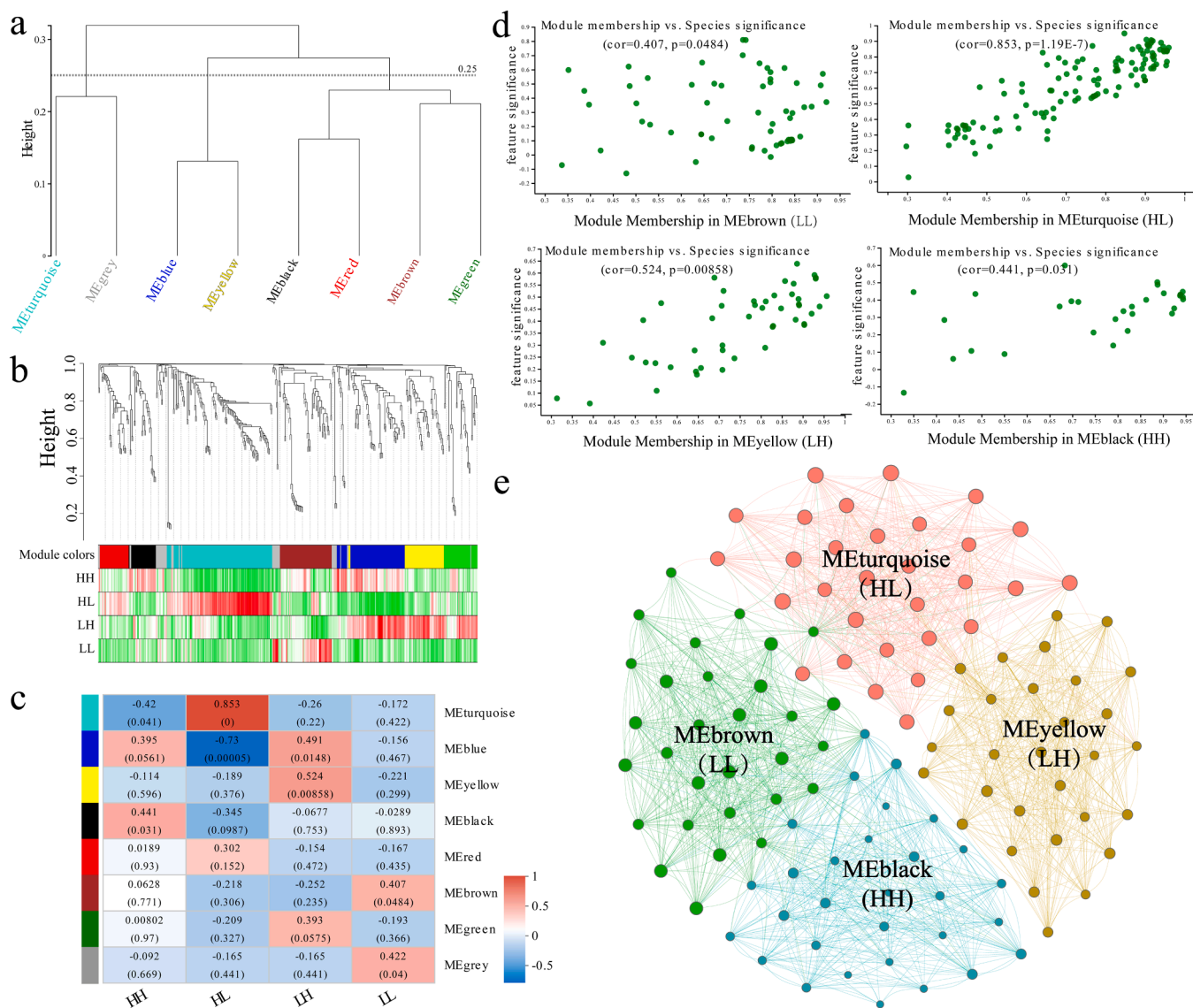


Fig. 5. WGCNA of bacterioplankton genes. (a) Module cluster dendrogram; (b and c) correlation between modules and features; (d) MM-GS analysis; (e) modular visualization of the co-occurrence network.

four treatment groups (Fig. 2). The networks of mutualism and antagonism were influenced primarily by Proteobacteria, whereas those of aggression and altruism were dominated by Cyanobacteria (Figs. 3 and 4). These findings highlight the adaptability of Proteobacteria, Bacteroidetes, and Cyanobacteria to diverse habitats (Du et al., 2022) and their responsiveness to changes in climate and nutrient loading, which significantly alters aquatic bacterioplankton composition and reduces biodiversity (Ryan et al. 2017), most notably by driving the occurrence of harmful algal blooms (Gobler, 2020). Notably, Cyanobacteria, especially *R. raciborskii*, are known for their adaptability to various environmental conditions and their competitive advantage over other phytoplankton species (Wu et al., 2022). Cyanobacteria such as *R. raciborskii* can efficiently use existing resources, withstand adverse conditions and form algae blooms more easily in freshwater (Bai et al., 2014; Briand et al., 2002; Burford et al., 2016). Because *R. raciborskii* can adapt to low temperatures by regulating metabolic pathways, growth morphology or akinete production (Huisman et al., 2018; Zheng et al., 2023), when the total phosphorus concentration in the water column reaches 0.02 mg l^{-1} , these conditions significantly promote *R. raciborskii* overgrowth and can trigger a bloom event (Burford et al., 2016). Therefore, in this study, significant differences in the density of

R. raciborskii were observed among the different treatment groups ($P < 0.05$, Fig. 1a), especially in the HL group.

The species diversity and species richness in the HL group were significantly different compared to those of other groups (Fig. 1g and h). This indicates that high cyanobacterial abundance typically decreases biodiversity (Zhang et al., 2021), which weakens the complexity and stability of microbial networks (Widder et al., 2014). Our network analysis also revealed a significant increase in the complexity and stability of the networks under warming conditions (Yuan et al., 2021; Zheng et al., 2024), particularly in the LH and HH treatment groups, where the number of nodes and edges exceeded those in the LL and HL treatment groups (Figs. 2 and 3). A possible reason is that greater species diversity under high-temperature conditions (Fig. 1g) increases the stability of the network (Lezcano et al., 2017; Zhang et al., 2021). The distribution of 22 key species identified as connectors and module hubs through Zi-Pi analysis revealed significant variability across treatments, with four module hubs belonging to *Raphidiopsis*, particularly in the HL group, where bloom intensity was greatest (Fig. S3). These keystone species, which serve as critical nodes within and between network modules, are pivotal in sustaining cyanobacterial bloom events (Ling et al., 2016). Our NMDS and ANOSIM analyses further validated the

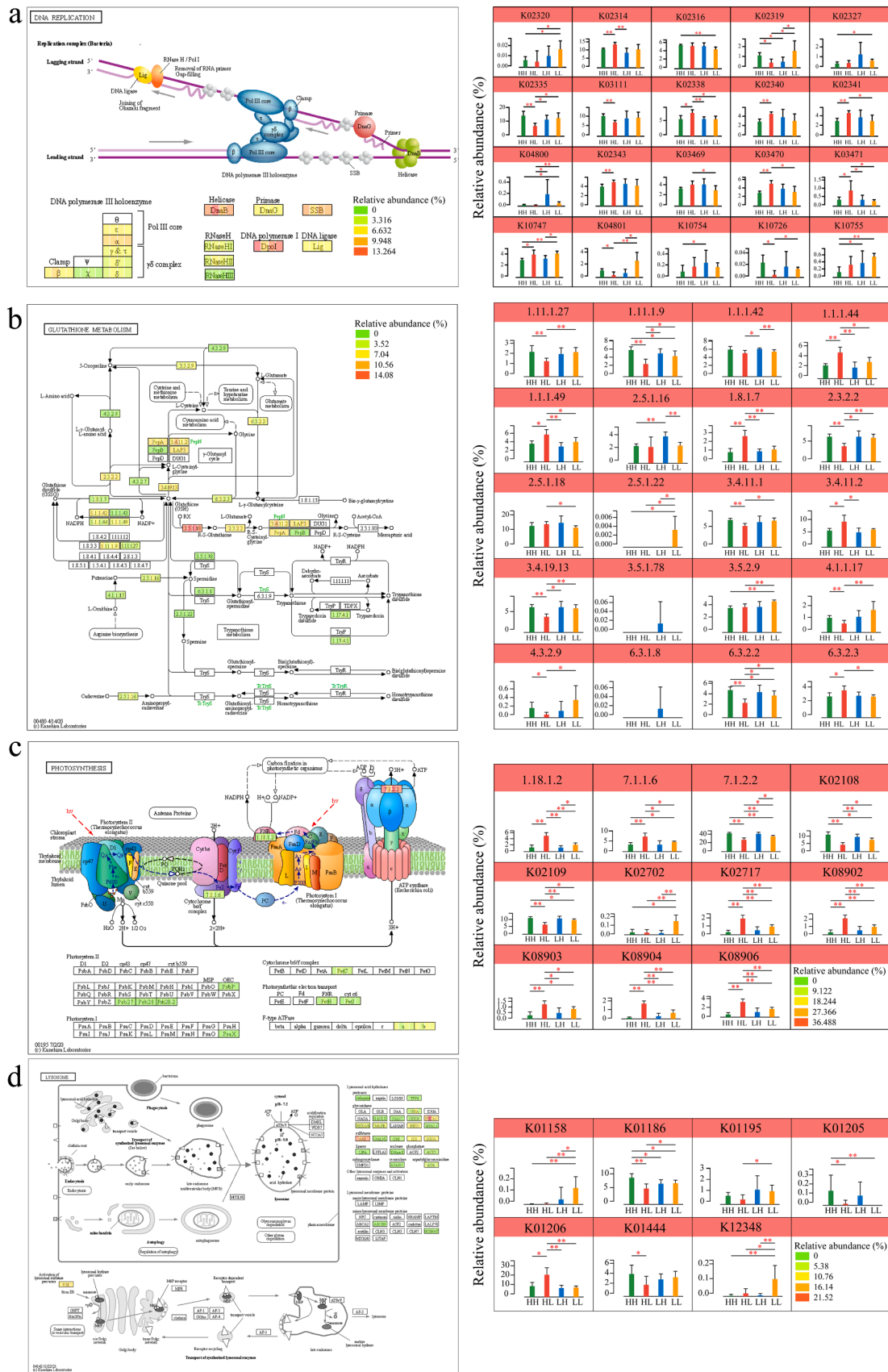


Fig. 6. Analysis of the differential expression of genes in metabolic pathways. (a–d) Top to bottom: Hub KEGG tertiary metabolic pathways and differentially expressed genes in the LL, LH, HL, and HH treatment groups. Each bar graph to the right of each pathway shows significant differences in gene transcription in the corresponding pathway among the different treatment groups.

significant influence of temperature and phosphorus changes on the bacterioplankton community composition ($P < 0.05$, Fig. 1i, Table S3), which is similar to the findings of Rigosi et al. (2014), who reported that climate warming and eutrophication altered cyanobacterial biomass and varied depending on the trophic state and microbial taxa of the lake. These results support our Hypothesis H1.

4.2. The synergistic effect of temperature and nutrient loading alters *R. raciborskii* blooms

Cyanobacterial blooms have become an important problem affecting the health of aquatic ecosystems (Du et al., 2022), and their occurrence is closely linked to climate change and water nutrient loading (Huisman et al., 2018). Excessive inputs of nutrients, such as phosphorus and nitrogen, are major contributors to outbreaks of cyanobacterial blooms (Luerling and Faassen, 2012). Although limiting these nutrients can effectively control and prevent cyanobacterial blooms (Shatwell and Köhler, 2019; Wang et al., 2018), our experiments indicate that *R. raciborskii* blooms occurred under both high- and low-phosphorus conditions (Fig. 1a). This finding is consistent with the findings of Reint et al. (2021), who reported that reducing nutrient loading was not effective in reducing cyanobacterial blooms. Wu et al. (2012) and Poselt et al. (2009) reported that increased phosphorus concentrations favor the formation of *R. raciborskii* blooms, noting the ability of *R. raciborskii* to utilize organic phosphorus sources efficiently and thrive under phosphorus-deficient conditions (Bai et al., 2014; Bonilla et al., 2012). *R. raciborskii* is considered a characteristic species of the tropics and subtropics (Neill et al., 2002). Elevated temperatures can promote the spread of *R. raciborskii* or outbreaks of cyanobacterial blooms (Briand et al., 2002; Wiedner et al., 2007). However, Jia et al. (2021) reported that *R. raciborskii* can still form blooms in West Lake in Yunnan at 15 °C. Our results revealed *R. raciborskii* blooms in all the treatment groups (Fig. 1a), partially supporting previous results.

The interaction between temperature and nutrient salts plays a crucial role in modulating the tolerance of cyanobacteria to varying nutrient conditions (Galvanese et al., 2019; Thrane et al., 2017), suggesting that the combined effects of these factors might differ from the effects of each individual factor. Multivariate analysis shows that temperature and phosphorus concentration have significant main effects on the density of *R. raciborskii*, in addition to an interaction effect between these two factors (Fig. 1b, Table S2). From an ecological perspective, this confirms that the growth of this cyanobacterium is highly sensitive to environmental temperature, consistent with its tropical origin and known thermal preference (Neill et al., 2002). The significant interaction between phosphorus and temperature suggests that nutrient availability modulates the effect of temperature. This is crucial, as in natural systems, temperature increases due to climate change could intensify nutrient-driven eutrophication, potentially leading to more intense or frequent cyanobacterial blooms. Our results are consistent with a wide range of ecological research showing that temperature and nutrient levels are fundamental factors controlling algal population dynamics (Huisman et al., 2018). In our study, *R. raciborskii* presented a relatively high relative abundance in both the LL and HH groups (Fig. 1c and e). On the one hand, higher temperatures generally favor cyanobacteria, particularly toxin-producing genera known for forming dense blooms in freshwater (Joehnk et al., 2008), with *R. raciborskii* deriving more benefits from elevated temperatures than other cyanobacteria do (Mehner et al., 2010). On the other hand, studies have shown that low phosphorus and low temperature are more favorable and allow *R. raciborskii* to successfully compete with other microorganisms (O'Neil et al., 2012; Zheng et al., 2023). A similar result was confirmed by the transcription of functional genes, with significantly more phosphorus transporters in the LL treatment groups than in the other treatment groups ($P < 0.05$, Table S16). These findings suggest that *R. raciborskii* might have a competitive advantage over the other cyanobacteria or bacterioplankton in the LL and HH groups.

Eutrophication (Beaulieu et al., 2013) and global warming (O'Neil et al., 2012; Paerl and Huisman, 2008) have long been recognized as significant drivers of cyanobacterial bloom occurrences, which is consistent with our findings that temperature, phosphorus, and their interactions significantly affect the growth of *R. raciborskii* (Table S2). However, Richardson et al. (2019) reported that the combination of elevated temperatures and high nutrient levels actually reduced cyanobacterial abundance. In our study, under low-phosphorus conditions, elevated temperatures promoted algal growth, whereas under high-phosphorus conditions, increased temperatures inhibited algal growth (Fig. 1b). Moreover, *R. raciborskii* blooms were an order of magnitude greater in the HL group than in the HH group (Fig. 1a), suggesting that cyanobacteria are more susceptible to blooms in low-temperature eutrophic waters because of their flexible adaptive strategies (Reint et al., 2021 and 2023). Interestingly, these findings contradict the results of most studies, which indicate that high temperatures and high phosphorus levels favor the occurrence of blooms (Carey et al., 2012; Paerl and Huisman, 2008; Taranu et al., 2012). Several factors may explain this discrepancy. Richardson et al. (2019) suggested that this discrepancy may be related to the high productivity in mesocosms caused by high nutrient loadings, with eutrophication and warming exacerbating the depletion of soluble inorganic carbon and carbon limitation in the water column reducing the abundance of cyanobacteria. Ryan et al. (2017) argued that much of the evidence for these results comes from observations or physiological measurements based on individual cultures, ignoring interspecies interactions. We believe this may also be related to the fact that eukaryotic algae are not counted. For example, Ryan et al. (2017) reported that green algae are more productive than cyanobacteria under high-temperature and high-phosphorus conditions. In summary, our results not only support our hypothesis (H2) but also further revised and supplemented it. The synergistic effect of temperature and nutrient loading increased the competitive advantage of *R. raciborskii* in the community for dominance, and the antagonistic effect of temperature and nutrient loading promoted the occurrence of *R. raciborskii* blooms.

4.3. Mechanisms of *R. raciborskii* blooms caused by temperature and nutrient loading

In aquatic ecosystems, algal blooms are typically associated with complex microbial interactions that are highly sensitive to environmental changes (Amin et al., 2015; Tanabe et al., 2023; Faust and Raes, 2012). Using a microbial behavioral ecology model, we investigated the symbiotic patterns between *R. raciborskii* and planktonic bacteria under various environmental conditions and their impact on bloom dynamics (Figs. 3 and 4). The results revealed a dominance of altruistic interactions (Fig. S4), consistent with findings by Du et al. (2022), which also highlighted the diversity of interactions between cyanobacteria and microbial communities. In the treatment group with the highest *R. raciborskii* bloom intensity (HL), cyanobacteria presented the greatest relative abundance in the mutualistic and antagonistic networks but the lowest relative abundance in the aggression networks (Fig. 3). This reflects their strategy of maintaining high growth rates and competitiveness through resource exchange and defense mechanisms, suggesting that microbes may exploit mutualistic relationships to obtain essential nutrients while protecting resources through antagonistic behaviors. Conversely, a reduction in aggressive behaviors indicates the establishment of ecological dominance through stable interactions, reducing the reliance on direct attacks as a strategy (Gerphagnon et al., 2015). Under the lowest bloom intensity conditions (HH), an imbalance in relative abundance between cyanobacteria and non-cyanobacteria likely led to resource competition and forced species to rely on aggressive survival strategies. This is a benign interaction and is influenced by environmental factors (Smith et al., 2021).

Studies by Shi and Falkowski (2008) demonstrated that environmental shifts influence microbial structure and function, initiating

adaptive changes in gene expression and metabolite synthesis (Kashtan et al., 2014). Specifically, in the HL group, there was a significant enrichment of enzymes and genes related to energy metabolism; photosynthesis; and the carbon, nitrogen, phosphorus, and sulfur cycles (Figs. 6C and S8–S10, Tables S7–S9 and S12–S15). These factors play crucial roles in maintaining cellular energy metabolism, redox balance, and normal cell function, thereby promoting cyanobacteria growth and exacerbating *R. raciborskii* blooms (Rohmer, 1999; Du et al., 2022). Under high-phosphate and high-temperature conditions (HH), the enrichment of lysosomal and related genes helps cope with cellular stress (Fig. 6d, Tables S7–S9), maintaining cellular homeostasis but at the expense of energy, possibly generating toxic byproducts through processes such as autophagy and metabolite degradation, ultimately suppressing cyanobacterial growth and reproduction (Lawrence and Zoncu, 2019; Settembre et al., 2013; Nakashima et al., 2006; Demuez et al., 2015). Therefore, changes in adaptive gene expression and optimized nutrient cycling reflect the self-regulation of planktonic bacteria under the dual pressures of climate change and nutrient loading (Shi and Falkowski, 2008; Kashtan et al., 2014). Our results not only support our hypothesis (H3), but also demonstrate the dynamic interaction between temperature and phosphorus in influencing the growth of *R. raciborskii* through multivariate analysis. From an ecological perspective, this interaction suggests that the influence of nutrient and temperature fluctuations on bloom dynamics is not static but varies over time, perhaps related to seasonal changes or episodic events, such as nutrient pulses from rainwater runoff. This result highlights the importance of considering temporal variability when predicting bloom occurrences (Cottingham et al., 2020). These results deepen our understanding of microbial ecological adaptation in complex environments and provide important insights and guidelines for the prevention and ecological restoration of algal blooms. We can develop more targeted strategies to prevent and control harmful cyanobacterial blooms, particularly in the context of global climate change and eutrophication.

5. Conclusion

This study reveals the effects of temperature and nutrient loading on *R. raciborskii* blooms through a comprehensive analysis of microbial communities. The synergistic effects of climate and nutrient variations enhance the competitive dominance of *R. raciborskii* within the cyanobacterial community, promoting aggressive behaviors among cyanobacterial species. The antagonistic effects of climate and nutrient changes particularly favor *R. raciborskii* bloom outbreaks, especially in eutrophic water bodies at approximately 20 °C. In addition, warming and increased species diversity enhance network complexity and stability. Proteobacteria and cyanobacteria are highly abundant in bacterial networks and behavioral ecological models. Proteobacteria are usually the dominant taxa in mutualistic and antagonistic relationships, whereas cyanobacteria are the dominant taxa in aggressive and altruistic relationships; in particular, *Raphidiopsis* in the Cyanobacteria phylum is the key hub species of the bacterial community. Altruism, dominated by Cyanobacteria, plays a leading role in microbial interactions, and various bacterial taxa contribute to the formation of bloom events through interspecies cooperation, with non-cyanobacterial bacteria playing an important role in this process. Microorganisms can adapt to environmental changes by regulating metabolic pathways and gene expression to achieve self-regulation in response to the dual pressures of temperature and nutrient loading. These findings are very important for the prevention and ecological restoration of aquatic blooms. In future research, integrating multivariate analyses to study the combined effects of complex microbial and environmental factors may reveal key mechanisms to address global climate change and provide new approaches to tackle related ecological challenges.

CRedit authorship contribution statement

Baohai Zheng: Writing – review & editing, Writing – original draft, Methodology, Investigation, Formal analysis, Conceptualization. **Ling Zhou:** Investigation, Formal analysis. **Jinna Wang:** Investigation, Data curation. **Peichang Dong:** Investigation, Formal analysis, Data curation. **Teng Zhao:** Data curation. **Yuting Deng:** Data curation. **Lirong Song:** Writing – review & editing. **Junqiong Shi:** Investigation. **Zhongxing Wu:** Writing – review & editing, Supervision, Funding acquisition, Conceptualization.

Declaration of competing interest

The authors declare that they have no known competing financial interests or personal relationships that could have appeared to influence the work reported in this paper.

Acknowledgments

The research was supported by the National Natural Science Foundation of China (nos. 42177055, 42477057).

Supplementary materials

Supplementary material associated with this article can be found, in the online version, at doi:10.1016/j.watres.2024.122725.

Data availability

Data will be made available on request.

References

- Amin, S.A., Hmelo, L.R., van Tol, H.M., Durham, B.P., Carlson, L.T., Heal, K.R., Morales, R.L., Berthiaume, C.T., Parker, M.S., Djunaedi, B., Ingalls, A.E., Parsek, M. R., Moran, M.A., Armbrust, E.V., 2015. Interaction and signalling between a cosmopolitan phytoplankton and associated bacteria. *Nature* 522 (7554), 98–U253.
- Anneville, O., Gammeter, S., Straile, D., 2005. Phosphorus decrease and climate variability: mediators of synchrony in phytoplankton changes among European alpine lakes. *Freshwater Biol.* 50 (10), 1731–1746.
- ANZECC, A., 2000. Australian and New Zealand Guidelines For Fresh Andmarine Water Quality, 1. Australian New Zealand Environment Conservation Council Agriculture Resource Management Council of Australia New Zealand Entomologist, Canberra.
- Bai, F., Liu, R., Yang, Y., Ran, X., Shi, J., Wu, Z., 2014. Dissolved organic phosphorus use by the invasive freshwater diazotroph cyanobacterium, *Cylindrospermopsis raciborskii*. *Harmf. Algae* 39, 112–120.
- Beaulieu, M., Pick, F., Gregory-Eaves, I., 2013. Nutrients and water temperature are significant predictors of cyanobacterial biomass in a 1147 lakes data set. *Limnol. Oceanogr.* 58 (5), 1736–1746.
- Bonilla, S., Aubriot, L., Soares, M.C.S., Gonzalez-Piana, M., Fabre, A., Huszar, V.L.M., Lurling, M., Antoniadis, D., Padsak, J., Kruk, C., 2012. What drives the distribution of the bloom-forming cyanobacteria *Planktothrix agardhii* and *Cylindrospermopsis raciborskii*? *FEMS Microbiol. Ecol.* 79 (3), 594–607.
- Bouma-Gregson, K., Olm, M.R., Probst, A.J., Anantharaman, K., Power, M.E., Banfield, J. F., 2019. Impacts of microbial assemblage and environmental conditions on the distribution of anatoxin-a producing cyanobacteria within a river network. *ISME J.* 13 (6), 1618–1634.
- Brauns, M., Allen, D.C., Boëchat, I.G., Cross, W.F., Ferreira, V., Graeber, D., Patrick, C.J., Peipoch, M., von Schiller, D., Gücker, B., 2022. A global synthesis of human impacts on the multifunctionality of streams and rivers. *Glob. Change Biol.* 28 (16), 4783–4793.
- Briand, J.F., Robillot, C., Quiblier-Lloberas, C., Humbert, J.F., Coute, A., Bernard, C., 2002. Environmental context of *Cylindrospermopsis raciborskii* (Cyanobacteria) blooms in a shallow pond in France. *Water Res.* 36 (13), 3183–3192.
- Burford, M.A., Beardall, J., Willis, A., Orr, P.T., Magalhaes, V.F., Rangel, L.M., Azevedo, S.M.F.O.E., Neilan, B.A., 2016. Understanding the winning strategies used by the bloom-forming cyanobacterium *Cylindrospermopsis raciborskii*. *Harmf. Algae* 54, 44–53.
- Carey, C.C., Ibelings, B.W., Hoffmann, E.P., Hamilton, D.P., Brookes, J.D., 2012. Ecophysiological adaptations that favour freshwater cyanobacteria in a changing climate. *Water Res.* 46 (5), 1394–1407.
- Cottingham, K.L., Weathers, K.C., Ewing, H.A., Greer, M.L., Carey, C.C., 2020. Predicting the effects of climate change on freshwater cyanobacterial blooms requires consideration of the complete cyanobacterial life cycle. *J. Plankton Res.* 43 (1), 10–19.

- Csardi, G., Nepusz, T., 2006. The igraph software package for complex network research. *Int. J. Compl. Syst.* 1695 (5), 1–9.
- Demuez, M., González-Fernández, C., Ballesteros, M., 2015. Algicidal microorganisms and secreted algicides: new tools to induce microalgal cell disruption. *Biotechnol. Adv.* 33 (8), 1615–1625.
- Du, C., Li, G., Xia, R., Li, C., Zhu, Q., Li, X., Li, J., Zhao, C., Tian, Z., Zhang, L., 2022. New insights into cyanobacterial blooms and the response of associated microbial communities in freshwater ecosystems. *Environ. Pollut.* 309, 119781.
- Elliott, J.A., 2012. Is the future blue-green? A review of the current model predictions of how climate change could affect pelagic freshwater cyanobacteria. *Water Res.* 46 (5), 1364–1371.
- Everson, S., Fabbro, L., Kinnear, S., Wright, P., 2011. Extreme differences in akinete, heterocyte and cylindrospermopsin concentrations with depth in a successive bloom involving *Aphanizomenon ovalisporum* (Forti) and *Cylindrospermopsis raciborskii* (Woloszynska) Seenaya and Subba Raju. *Harmf. Algae* 10 (3), 265–276.
- Faust, K., Raes, J., 2012. Microbial interactions: from networks to models. *Nat. Rev. Microbiol.* 10 (8), 538–550.
- Freeman, E.C., Creed, I.F., Jones, B., Bergström, A.-K., 2020. Global changes may be promoting a rise in select cyanobacteria in nutrient-poor northern lakes. *Glob. Change Biol.* 26 (9), 4966–4987.
- Galvane, E.F., Padial, A.A., Aubriot, L., 2019. Acclimation at high temperatures increases the ability of *Raphidiopsis raciborskii* (Cyanobacteria) to withstand phosphate deficiency and reveals distinct strain responses. *Eur. J. Phycol.* 54 (3), 359–368.
- Gerphagnon, M., Macarthur, D.J., Latour, D., Gachon, C.M.M., Van Ogtrop, F., Gleason, F.H., Sime-Ngando, T., 2015. Microbial players involved in the decline of filamentous and colonial cyanobacterial blooms with a focus on fungal parasitism. *Environ. Microbiol.* 17 (8), 2573–2587.
- Gobler, C.J., 2020. Climate Change and Harmful Algal Blooms: insights and perspective. *Harmf. Algae* 91.
- He, X., Zhang, Q., Li, B., Jin, Y., Jiang, L., Wu, R., 2021. Network mapping of root-microbe interactions in *Arabidopsis thaliana*. *npj Biofilm. Microbiom.* 7 (1), 72.
- Hu, H., Wei, Y., 2006. *The Freshwater Algae of China: systematics, Taxonomy and Ecology*. Science press, Beijing.
- Hu, J., Amor, D.R., Barbier, M., Bunin, G., Gore, J., 2022. Emergent phases of ecological diversity and dynamics mapped in microcosms. *Science* 378 (6615), 85–89.
- Huisman, J., Codd, G.A., Paerl, H.W., Ibelings, B.W., Verspagen, J.M.H., Visser, P.M., 2018. Cyanobacterial blooms. *Nat. Rev. Microbiol.* 16 (8), 471–483.
- Isabwe, A., Yang, J.R., Wang, Y., Liu, L., Chen, H., Yang, J., 2018. Community assembly processes underlying phytoplankton and bacterioplankton across a hydrologic change in a human-impacted river. *Sci. Total Environ.* 630, 658–667.
- Jia, N., Wang, Y., Guan, Y., Chen, Y., Li, R., Yu, G., 2021. Occurrence of *Raphidiopsis raciborskii* blooms in cool waters: Synergistic effects of nitrogen availability and ecotypes with adaptation to low temperature. *Environ. Pollut.* 270, 116070.
- Jiang, L., Liu, X., He, X., Jin, Y., Cao, Y., Zhan, X., Griffin, C.H., Gragnoli, C., Wu, R., 2021. A behavioral model for mapping the genetic architecture of gut-microbiota networks. *Gut Microb.* 13 (1), 1820847.
- Jiang, L., Xu, J., Sang, M., Zhang, Y., Ye, M., Zhang, H., Wu, B., Zhu, Y., Xu, P., Tai, R., Zhao, Z., Jiang, Y., Dong, C., Sun, L., Griffin, C.H., Gragnoli, C., Wu, R., 2019. A drive to driven model of mapping intraspecific interaction networks. *iScience* 22, 109–122.
- Joehnk, K.D., Huisman, J., Sharples, J., Sommeijer, B., Visser, P.M., Stroom, J.M., 2008. Summer heatwaves promote blooms of harmful cyanobacteria. *Glob. Change Biol.* 14 (3), 495–512.
- Kashtan, N., Roggensack, S.E., Rodrigue, S., Thompson, J.W., Biller, S.J., Coe, A., Ding, H., Marttinen, P., Malmstrom, R.R., Stocker, R., Follows, M.J., Stepanauskas, R., Chisholm, S.W., 2014. Single-cell genomics reveals hundreds of coexisting subpopulations in wild prochlorococcus. *Science* 344 (6182), 416–420.
- Kehoe, M., O'Brien, K.R., Grinham, A., Burford, M.A., 2015. Primary production of lake phytoplankton, dominated by the cyanobacterium *Cylindrospermopsis raciborskii*, in response to irradiance and temperature. *Inland Water.* 5 (2), 93–100.
- Kong, L., Feng, Y., Du, W., Zheng, R., Sun, J., Rong, K., Sun, W., Liu, S., 2023. Cross-Feeding between Filamentous Cyanobacteria and Symbiotic Bacteria Favors Rapid Photogranulation. *Environ. Sci. Technol.* 57 (44), 16953–16963.
- Langfelder, P., Horvath, S., 2008. WGCNA: an R package for weighted correlation network analysis. *BMC Bioinf.* 9 (1), 559.
- Lawrence, R.E., Zoncu, R., 2019. The lysosome as a cellular centre for signalling, metabolism and quality control. *Nat. Cell Biol.* 21 (2), 133–142.
- Lezcano, M.Á., Velázquez, D., Quesada, A., El-Shehaw, R., 2017. Diversity and temporal shifts of the bacterial community associated with a toxic cyanobacterial bloom: an interplay between microcystin producers and degraders. *Water Res.* 125, 52–61.
- Li, K., Cheng, K., Wang, H., Zhang, Q., Yang, Y., Jin, Y., He, X., Wu, R., 2022. Disentangling leaf-microbiome interactions in *Arabidopsis thaliana* by network mapping. *Front. Plant Sci.* 13.
- Ling, N., Zhu, C., Xue, C., Chen, H., Duan, Y., Peng, C., Guo, S., Shen, Q., 2016. Insight into how organic amendments can shape the soil microbiome in long-term field experiments as revealed by network analysis. *Soil Biol. Biochem.* 99, 137–149.
- Liu, L., Chen, H., Liu, M., Yang, J.R., Xiao, P., Wilkinson, D.M., Yang, J., 2019. Response of the eukaryotic plankton community to the cyanobacterial biomass cycle over 6 years in two subtropical reservoirs. *ISME J.* 13 (9), 2196–2208.
- Luerling, M., Faassen, E.J., 2012. Controlling toxic cyanobacteria: effects of dredging and phosphorus-binding clay on cyanobacteria and microcystins. *Water Res.* 46 (5), 1447–1459.
- Mammides, C., 2020. A global assessment of the human pressure on the world's lakes. *Glob. Environ. Change* 63, 102084.
- Mehner, G., Leunert, F., Cirés, S., Jöhnk, K.D., Rüdiger, J., Nixdorf, B., Wiedner, C., 2010. Competitiveness of invasive and native cyanobacteria from temperate freshwaters under various light and temperature conditions. *J. Plankton Res.* 32 (7), 1009–1021.
- Mohamed, Z.A., 2016. Harmful cyanobacteria and their cyanotoxins in Egyptian fresh waters – state of knowledge and research needs. *Afr. J. Aquat. Sci.* 41 (4), 361–368.
- Nakashima, T., Miyazaki, Y., Matsuyama, Y., Muraoka, W., Yamaguchi, K., Oda, T., 2006. Producing mechanism of an algicidal compound against red tide phytoplankton in a marine bacterium γ -proteobacterium. *Appl. Microbiol. Biotechnol.* 73 (3), 684–690.
- Neill, S.J., Desikan, R., Clarke, A., Hurst, R.D., Hancock, J.T., 2002. Hydrogen peroxide and nitric oxide as signalling molecules in plants. *J. Exp. Bot.* 53 (372), 1237–1247.
- Newton, R.J., Jones, S.E., Eiler, A., McMahon, K.D., Bertilsson, S., 2011. A guide to the natural history of freshwater lake bacteria. *Microbiol. Molec. Biol. Rev.* 75 (1), 14–49.
- O'Brien, K.R., Burford, M.A., Brookes, J.D., 2009. Effects of light history on primary productivity in a phytoplankton community dominated by the toxic cyanobacterium *Cylindrospermopsis raciborskii*. *Freshwater Biol.* 54 (2), 272–282.
- O'Neil, J.M., Davis, T.W., Burford, M.A., Gobler, C.J., 2012. The rise of harmful cyanobacteria blooms: the potential roles of eutrophication and climate change. *Harmf. Algae* 14, 313–334.
- Ohtani, I., Moore, R.E., Runnegar, M.T.C., 1992. Cylindrospermopsin: a potent hepatotoxin from the blue-green alga. *J. Am. Chem. Soc.* 114 (20), 7941–7942.
- Ou-yang, T., Yang, S., Zhao, L., Ji, L., Shi, J., Wu, Z., 2022. Temporal heterogeneity of bacterial communities and their responses to *Raphidiopsis raciborskii* blooms. *Microbiol. Res.* 262, 127098.
- Paerl, H.W., Huisman, J., 2008. Blooms like it hot. *Science* 320 (5872), 57–58.
- Polazzo, F., dos Anjos, T.B.O., Arenas-Sánchez, A., Romo, S., Vighi, M., Rico, A., 2022. Effect of multiple agricultural stressors on freshwater ecosystems: the role of community structure, trophic status, and biodiversity-functioning relationships on ecosystem responses. *Sci. Total Environ.* 807, 151052.
- Posselt, A.J., Burford, M.A., Shaw, G., 2009. Pulses of phosphate promote dominance of the toxic cyanophyte *Cylindrospermopsis raciborskii* in a subtropical water reservoir. *J. Phycol.* 45 (3), 540–546.
- Reinl, K.L., Brookes, J.D., Carey, C.C., Harris, T.D., Ibelings, B.W., Morales-Williams, A. M., De Senerpont Domis, L.N., Atkins, K.S., Isles, P.D.F., Mesman, J.P., North, R.L., Rudstam, L.G., Stelzer, J.A.A., Venkiteswaran, J.J., Yokota, K., Zhan, Q., 2021. Cyanobacterial blooms in oligotrophic lakes: shifting the high-nutrient paradigm. *Freshwater Biol.* 66 (9), 1846–1859.
- Reinl, K.L., Harris, T.D., North, R.L., Almela, P., Berger, S.A., Bizic, M., Burnet, S.H., Grossart, H.-P., Ibelings, B.W., Jakobsson, E., Knoll, L.B., Lafrancois, B.M., McElarney, Y., Morales-Williams, A.M., Obertegger, U., Ogashawara, I., Paule-Mercado, M.C., Peierls, B.L., Rusak, J.A., Sarkar, S., Sharma, S., Trout-Haney, J.V., Urrutia-Cordero, P., Venkiteswaran, J.J., Wain, D.J., Warner, K., Weyhenmeyer, G. A., Yokota, K., 2023. Blooms also like it cold. *Limnol. Oceanogr. Lett.* 8 (4), 546–564.
- Richardson, J., Feuchtmayr, H., Miller, C., Hunter, P.D., Maberly, S.C., Carvalho, L., 2019. Response of cyanobacteria and phytoplankton abundance to warming, extreme rainfall events and nutrient enrichment. *Glob. Change Biol.* 25 (10), 3365–3380.
- Rigosi, A., Carey, C.C., Ibelings, B.W., Brookes, J.D., 2014. The interaction between climate warming and eutrophication to promote cyanobacteria is dependent on trophic state and varies among taxa. *Limnol. Oceanogr.* 59 (1), 99–114.
- Rippka, R., Deruelles, J., Waterbury, J.B., Herdman, M., Stanier, R.Y., 1979. Generic Assignments, Strain Histories and Properties of Pure Cultures of Cyanobacteria. *Microbiology* 111 (1), 1–61.
- Rohmer, M., 1999. The discovery of a mevalonate-independent pathway for isoprenoid biosynthesis in bacteria, algae and higher plants. *Nat. Prod. Rep.* 16 (5), 565–574.
- Ryan, C.N., Thomas, M.K., Litchman, E., 2017. The effects of phosphorus and temperature on the competitive success of an invasive cyanobacterium. *Aquat. Ecol.* 51 (3), 463–472.
- Saleem, M., Hu, J., Jousset, A., 2019. Annual Review of Ecology, Evolution, and Systematics, 50, pp. 145–168. Futuyma, D.J. (ed).
- Schloss, P.D., Westcott, S.L., Ryabin, T., Hall, J.R., Hartmann, M., Hollister, E.B., Lesniewski, R.A., Oakley, B.B., Parks, D.H., Robinson, C.J., Sahl, J.W., Stres, B., Thallinger, G.G., Van Horn, D.J., Weber, C.F., 2009. Introducing mothur: open-source, platform-independent, community-supported software for describing and comparing microbial communities. *Appl. Environ. Microbiol.* 75 (23), 7537–7541.
- Settembre, C., Fraldi, A., Medina, D.L., Ballabio, A., 2013. Signals from the lysosome: a control centre for cellular clearance and energy metabolism. *Nat. Rev. Mol. Cell Biol.* 14 (5), 283–296.
- Shao, K., Zhang, L., Wang, Y., Yao, X., Tang, X., Qin, B., Gao, G., 2014. The responses of the taxa composition of particle-attached bacterial community to the decomposition of *Microcystis* blooms. *Sci. Total Environ.* 488–489, 236–242.
- Shatwell, T., Köhler, J., 2019. Decreased nitrogen loading controls summer cyanobacterial blooms without promoting nitrogen-fixing taxa: long-term response of a shallow lake. *Limnol. Oceanogr.* 64 (S1), S166–S178.
- Shi, T., Falkowski, P.G., 2008. Genome evolution in cyanobacteria: the stable core and the variable shell. *Proc. Natl. Acad. Sci. U.S.A.* 105 (7), 2510–2515.
- Sinha, R., Pearson, L.A., Davis, T.W., Burford, M.A., Orr, P.T., Neilan, B.A., 2012. Increased incidence of *Cylindrospermopsis raciborskii* in temperate zones - Is climate change responsible? *Water Res.* 46 (5), 1408–1419.
- Smith, D.J., Tan, J.Y., Powers, M.A., Lin, X.N., Davis, T.W., Dick, G.J., 2021. Individual *Microcystis* colonies harbour distinct bacterial communities that differ by *Microcystis* oligotype and with time. *Environ. Microbiol.* 23 (9), 5652–5657.
- Stocker, T., 2014. Climate Change 2013: The Physical Science Basis: Working Group I contribution to the *Fifth assessment Report of the Intergovernmental Panel On Climate Change*. Cambridge university press, Cambridge.

- Tanabe, Y., Yamaguchi, H., Yoshida, M., Kai, A., Okazaki, Y., 2023. Characterization of a bloom-associated alphaproteobacterial lineage, 'Candidatus Phycosocius': insights into freshwater algal-bacterial interactions. *ISME Commun.* 3 (1).
- Taranu, Z.E., Zurawell, R.W., Pick, F., Gregory-Eaves, L., 2012. Predicting cyanobacterial dynamics in the face of global change: the importance of scale and environmental context. *Glob. Change Biol.* 18 (12), 3477–3490.
- Te, S.H., Kok, J.W.K., Luo, R., You, L., Sukarji, N.H., Goh, K.C., Sim, Z.Y., Zhang, D., He, Y., Gin, K.Y.-H., 2023. Coexistence of synechococcus and microcystis blooms in a tropical urban reservoir and their links with microbiomes. *Environ. Sci. Technol.* 57 (4), 1613–1624.
- Thrane, J.-E., Hessen, D.O., Andersen, T., 2017. Plasticity in algal stoichiometry: experimental evidence of a temperature-induced shift in optimal supply N:P ratio. *Limnol. Oceanogr.* 62 (4), 1346–1354.
- Wang, K., Razzano, M., Mou, X., 2020. Cyanobacterial blooms alter the relative importance of neutral and selective processes in assembling freshwater bacterioplankton community. *Sci. Total Environ.* 706, 135724.
- Wang, S., Xiao, J., Wan, L., Zhou, Z., Wang, Z., Song, C., Zhou, Y., Cao, X., 2018. Mutual dependence of nitrogen and phosphorus as key nutrient elements: one facilitates *dolichospermum flos-aquae* to overcome the limitations of the other. *Environ. Sci. Technol.* 52 (10), 5653–5661.
- Widder, S., Besemer, K., Singer, G.A., Ceola, S., Bertuzzo, E., Quince, C., Sloan, W.T., Rinaldo, A., Battin, T.J., 2014. Fluvial network organization imprints on microbial co-occurrence networks. *Proceed Natl. Acad. Sci.* 111 (35), 12799–12804.
- Willis, A., Chuang, A.W., Woodhouse, J.N., Neilan, B.A., Burford, M.A., 2016. Intraspecific variation in growth, morphology and toxin quotas for the cyanobacterium, *Cylindrospermopsis raciborskii*. *Toxicon* 119, 307–310.
- Wu, Z., Yang, S., Shi, J., 2022. Overview of the distribution and adaptation of a bloom-forming cyanobacterium *Raphidiopsis raciborskii*: integrating genomics, toxicity, and ecophysiology. *J. Oceanol. Limnol.* 40 (5), 1774–1791.
- Wu, Z., Zeng, B., Li, R., Song, L., 2012. Physiological regulation of *Cylindrospermopsis raciborskii* (Nostocales, Cyanobacteria) in response to inorganic phosphorus limitation. *Harmf. Algae* 15, 53–58.
- Yuan, M.M., Guo, X., Wu, L., Zhang, Y., Xiao, N., Ning, D., Shi, Z., Zhou, X., Wu, L., Yang, Y., Tiedje, J.M., Zhou, J., 2021. Climate warming enhances microbial network complexity and stability. *Nat. Clim. Change* 11 (4), 343–U100.
- Zhang, Z., Fan, X., Peijnenburg, W.J.G.M., Zhang, M., Sun, L., Zhai, Y., Yu, Q., Wu, J., Lu, T., Qian, H., 2021. Alteration of dominant cyanobacteria in different bloom periods caused by abiotic factors and species interactions. *J. Environ. Sci.* 99, 1–9.
- Zheng, B., Dong, P., Zhao, T., Deng, Y., Li, J., Song, L., Wang, J., Zhou, L., Shi, J., Wu, Z., 2024. Strategies for regulating the intensity of different cyanobacterial blooms: insights from the dynamics and stability of bacterioplankton communities. *Sci. Total Environ.* 918, 170707.
- Zheng, B., He, S., Zhao, L., Li, J., Du, Y., Li, Y., Shi, J., Wu, Z., 2023. Does temperature favour the spread of *Raphidiopsis raciborskii*, an invasive bloom-forming cyanobacterium, by altering cellular trade-offs? *Harmf. Algae* 124, 102406.